Hindawi
Advances in Materials Science and Engineering
Volume 2021, Article ID 6627395, 14 pages
https://doi.org/10.1155/2021/6627395

*Research Article*

# Simulation Research on the Influence of the Clearance to the Impact Contact Characteristics between Coal Gangue and the Clearance-Contained Tail Beam Structure

**Yang Yang**[1], **Zhengyuan Xin**[1], **Qingliang Zeng**[1,2] and **Zhihai Liu**[3]

[1]*College of Mechanical and Electronic Engineering, Shandong University of Science and Technology, Qingdao 266590, China*
[2]*College of Information Science and Engineering, Shandong Normal University, Jinan 250358, China*
[3]*College of Transportation, Shandong University of Science and Technology, Qingdao 266590, China*

Correspondence should be addressed to Zhihai Liu; zhihliu@sdust.edu.cn

Received 30 October 2020; Revised 22 December 2020; Accepted 2 January 2021; Published 23 January 2021

Academic Editor: Georgios I. Giannopoulos



There are various forms of clearance at the connection of various parts of the hydraulic support. However, the influence of clearance has been ignored in various related research studies of the hydraulic support. In order to clearly grasp the accurate impact contact response law between coal gangue and the hydraulic support, the radial clearance in the pin shaft connection structure of the tail beam is considered for the first time in this paper. By constructing the theoretical contact model of the pin shaft connection, the difficulty of studying the interaction between coal gangue and the hydraulic support through theoretical solution is proved. On this basis, the finite element contact simulation analysis method is proposed to study the impact contact behavior between coal gangue and the tail beam. This paper constructed the finite element impacting simulation model between coal gangue and the radial clearance-contained tail beam structure and carried out impact contact simulation between coal gangue and the multiple clearance-contained tail beam structure as well as the changing clearance-contained tail beam structure, respectively, and contact responses of the tail beam structure such as the spring stress, the pin shaft test point stress, acceleration, and velocity of the tail beam test point under different working conditions are obtained. The influence law of clearance on different contact responses is studied, and the differences of contact responses after coal gangue impact between two clearance-contained tail beam structures and three clearance-contained tail beam structures are compared and analyzed. Research results show that, in the condition of multiclearance, the amplitude of each contact response when gangue is impacted is greater than that of coal. When the radial clearance of the connection unit increases from 0 to 0.25 mm, the overall fluctuation amplitude of the contact responses decreases. In 3-clearance state, increase of the radial clearance size of the connection unit will lead to the increase of the spring stress, the stress of the pin shaft test point, and the velocity of the tail beam test point gradually and the decrease of the acceleration of the tail beam test point. Throughout the research, the vibration response of the pin shaft can be taken as coal gangue recognition parameter. The work provides a theoretical basis for the study of the influence law of clearance on hydraulic support and provides a reference for the study of contact behavior between coal gangue and the hydraulic support.

## 1. Introduction

Hydraulic support is the important supporting equipment in coal mining. In order to improve the service ability of the hydraulic support, many research studies have been carried out on the design, movement, and mechanical properties of the hydraulic support, as well as its service performance. Xu et al. [1] analyzed the force and motion characteristics of the face sprag of the hydraulic support, and the coupling effect between the face sprag and coal face is studied. Witek and Prusek [2] studied the performance of the two-legged shield support by numerical simulation and experimental test. Wang et al. [3] investigated the stress and stability of the double telescopic props of the hydraulic support. Xie et al. [4] analyzed the space bearing characteristics of the top beam of the four-pillar chock-shield support. Zhao et al. [5]

studied the fatigue performance of the box-welded structure in the hydraulic support. Ge et al. [6] investigated the support attitude adjustment method of the hydraulic support groups during propulsion. Wang et al. [7] established the mechanical model of the four-leg chock-shield hydraulic support and analyzed its adaptability and influencing factors. Guan et al. [8] designed the new type of hydraulic support with double parallelogram structure, and the dynamic response characteristics and the natural frequency of the prop and the balanced jack are analyzed. Tian et al. [9] designed a six-pillar backfilling hydraulic support, the differential equations of its motion and state space model are established, and the effects of disturbance frequency and amplitude on the vertical vibration and roll and pitch vibration of the top beam are studied. Szurgacz and Brodny [10] investigated the dynamic response of the prop of the hydraulic support under the impact of the falling body. A series of research provides guarantees for the application of hydraulic support in downhole. However, most of these studies focus on the movement and stress of the hydraulic support, reliability of the props, or the coupling effect between the hydraulic support and surrounding rock, and few studies involve the influence of atypical structure assembly parameters on the hydraulic support. In particular, there is little research on the clearance of the hydraulic support in the field of coal mining.

Clearance is widely existed in the mechanical structure, and domestic and foreign scholars have carried out a lot of in-depth research on the influence of the clearance nonlinear factor on the mechanism. Starting with a two-dimensional planar bar system, Ting et al. [11] studied the effect of the joint clearance on the position and attitude deviation of the connecting rod and manipulator and found that joint clearance would lead to the uncertainty in the position and direction of the mechanism. Wang et al. [12] studied the dynamic response of the planar four-bar mechanism with multiple clearance joints by theoretical modeling. Chunmei et al. [13] established a single degree of freedom dynamic model for the separation and collision process of the elastic linkage mechanism, and the results show that the stability of the mechanism with large radial clearance is much lower than that of the mechanism without clearance. Yang et al. [14] found that the clearance size was nonlinear and positively correlated with angular acceleration of the rocker and the joint contact force through the research of the RSSR mechanism. Flores and Ambrósio [15] believed that the joint clearance is the source of impact force, and the joint clearance will cause the abrasion of the joint and system performance degradation. Zhang et al. [16] found that the increase of the clearance value of the rotating pair will reduce the motion precision of the mechanism through the research of the parallelogram mechanism with clearance redundancy constraint. Zhang et al. [17] studied the dynamic characteristics of the 3-PRR planar parallel mechanism with clearance and the wear characteristics of the kinematic pairs through theoretical modeling. Shiau et al. [18] found that the system dynamic response and the joint contact force will increase with the increase of the joint clearance through the nonlinear dynamic analysis of the 3-PRS series and parallel mechanism. Li et al. [19] proposed a theoretical model of the planar space deployable mechanism with revolute joint clearance and studied the influence of the clearance and parameter uncertainty on its motion accuracy and dynamic performance. Erkaya and Uzmay [20] studied the influence of the joint clearance on the vibration and noise characteristics of the slider-crank mechanism, and the research showed that the clearance would lead to the degradation of the vibration characteristics and the deterioration of the dynamic performance of the mechanism and the increase of the clearance would lead to the increase of the vibration noise level and amplitude. Through the research of 3-RRR parallel mechanism, Zhang et al. [21] found that the node clearance had great influence on the displacement, velocity, acceleration, and driving moment of the platform, and the clearance would lead to the nonlinear vibration of the mechanism. Qiu et al. [22] found that the collision force of the clearance would accelerate the damage of the hinge through the research on the performance of windsurfing. Song et al. [23] proposed the modular dynamic modeling method to establish the theoretical model of the 3-RRR planar parallel mechanism and studied the influence of the kinematic pair clearance on the dynamic performance of the mechanism. Gu et al. [24] carried out the analysis of the floating space manipulator, and the research results showed that the joint clearance size would affect the output fluctuation amplitude and frequency of the manipulator and reduce its motion accuracy. Existing studies have fully confirmed that the existence of the clearance will greatly increase the dynamic characteristics of the mechanism and the dynamic stress of the components, causing the nonlinear vibration of the components and affecting the motion and dynamic response of the mechanism.

Top coal caving hydraulic support is the typical multibody assembly mechanical structure, and it is composed of multiple components such as the top beam, shield beam, tail beam, base, prop, tail beam jack, and flashboard, as shown in Figure 1. The key connection units between each component are mainly ball pair and pin shaft connection. The field survey results of the production enterprises show that, due to the limitations of machining accuracy and assembly conditions, the radial assembly clearances ranging from 2 mm to 10 mm and transverse assembly clearances ranging from 6 mm to 10 mm exist in the connecting units of the pin shaft and pin hole during the production of the hydraulic support. As the important supporting part, the existence of the clearance affects the stability, stress and bearing characteristics, and posture control of the hydraulic support and will bring a nonnegligible combination influence on its posture and movement. At the same time, with the development and progress of technology, many scholars in the field of engineering proposed structural optimization [25], optimum of algorithm [26–29], and the production process optimization method to improve the production capacity and efficiency of the series of engineering tools such as the equipment and algorithms. In the field of mining, in order to promote the optimization design and improvement of the hydraulic support, the influence of clearance on the hydraulic support must also be an in-depth exploration.

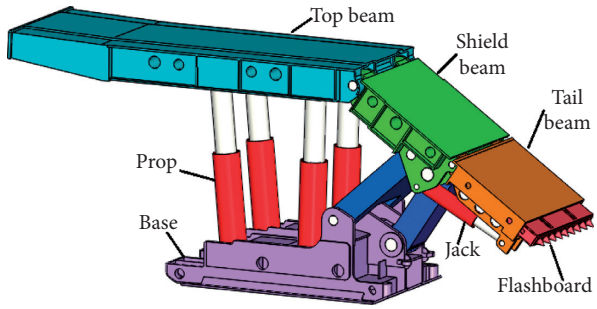


Figure 1: Assembly body of the top coal caving hydraulic support.

Therefore, the factor of clearance must be taken into account when the hydraulic support and its relevant series of research are studied. However, most of the above studies on the clearance of the mechanism are equivalent to the planar mechanism or space bar system, and the mostly adopted method is the theoretical modeling and then numerical simulation by iterative solution in the ideal state, in which the variation of the components' mass and bearing load with the position distribution is ignored in the research process and the influence of the spatial structure on the system dynamics is also ignored. Meanwhile, the flexibility of the material is also not sufficiently considered. The method of theoretical modeling is difficult to accurately calculate the unknown process of the clearance contact, such as the real-time variation of the contact process information, contact area, and contact point position. Therefore, the above research method ignoring many factors in the research will lead to the deviation between the research results and the actual situation. In the research relevant to the clearance of the hydraulic support, we should seek a method to consider more influencing factors and improve the research accuracy.

When we conducted the impact effect research between coal gangue and tail beam of the top coal caving hydraulic support in the relevant research of the hydraulic support, the nonlinear factor of clearance is introduced for the first time in this paper. Through the theoretical modeling for the single radial clearance connection unit of the tail beam and the analysis of the multiple clearances-contained tail beam structure, the difficulty for the system theoretical modeling and solution is studied and the finite element contact simulation is determined as the research method. On this basis, for further research on the interaction law between coal gangue and the multiple clearances-contained tail beam structure, the 3D finite element impact simulation model between coal gangue and the clearance-contained tail beam structure is established, and the impact contact simulation under the conditions of multiple clearances and variable clearances were conducted, respectively. Then, impact contact dynamic characteristics between coal gangue and the clearance-contained tail beam structure with different conditions are compared and analyzed. Finally, the influence law of the clearance to the contact response and the contact response differences of the impact between coal and gangue are obtained.

## 2. Difficulty Analysis for the System Theoretical Modeling and Solution

According to the definition of L-N nonlinear spring damping contact force model, the normal contact force between a sphere and a plane is composed of theoretical elastic force and damping force. The model can be expressed as follows [30–32]:

$$P_N = K \cdot \delta^n + D_n \cdot \dot{\delta}, \tag{1}$$

where $K$ is the contact stiffness, $n = 3/2$, $D_n$ is the damping coefficient, $\delta$ is the normal compression deformation, $\dot{\delta}$ is the normal contact velocity, and $e$ is the restitution coefficient.

Among them, the contact stiffness $K_W$ between external contacted objects can be expressed as [33–35]

$$K_W = \frac{4\sqrt{R_W}}{3E}, \tag{2}$$

$$E = \frac{1-\nu_1^2}{E_1} + \frac{1-\nu_2^2}{E_2}, \tag{3}$$

$$R_W = \frac{R_1 R_2}{R_1 + R_2}. \tag{4}$$

The contact stiffness $K_N$ between internal contacted objects can be expressed as [36–38]

$$K_N = \frac{4\sqrt{R_N}}{3\pi E}, \tag{5}$$

$$R_N = \frac{R_1 R_2}{|R_1 - R_2|}. \tag{6}$$

According to the modified Coulomb law, the tangential contact force [39–41] of the internal contact can be expressed as

$$P_t = -c_f c_d P_N \operatorname{sgn}(v_t), \tag{7}$$

in which

$$c_d = \begin{cases} 0, & |v_t| < v_0, \\ \dfrac{|v_t| - v_0}{v_1 - v_0}, & v_0 \le |v_t| \le v_1, \\ 1, & |v_t| > v_1, \end{cases} \tag{8}$$

where $R_1$, $E_1$, and $\nu_1$ and $R_2$, $E_2$, and $\nu_2$ are the radius, elastic modulus, and Poisson's ratio of at the contact point between two objects, respectively, $E$ is the equivalent elastic modulus, $R_W$ and $R_N$ are the equivalent contact radii of the external contact and internal contact, respectively, $c_d$ is the dynamic correction coefficient, $c_f$ is the frictional coefficient, $v_0$ and $v_1$ are given bounds for the tangential velocity, $v_t$ is the relative tangential velocity between the contact surfaces, and $|v_t|$ is the relative tangential speed.

Tail beam is mainly connected with the hydraulic support through the pin shaft. Among them, there are radial and lateral clearances at the connection units between the shield beam and the tail beam, between the tail beam and the tail beam jack, and between the tail beam jack and the shield beam. In order to simplify the analysis, ignoring the structure of the flashboard, the other parts of the hydraulic support are equivalent to the equivalent structure with the same support function to the tail beam, and the equivalent tail beam structure is obtained. The two-dimensional contact model of its radial clearance is shown in Figure 2. The outside clearance between the tail beam and the equivalent structure is defined as point 1, and this single clearance is taken as the research object. If we only consider the contact behavior at this clearance, it is formed by connecting an axle hole of the tail beam with two lugs of the equivalent structure through a pin shaft. As shown in Figure 3, under the impact of coal gangue, the tail beam will impact and contact with the pin shaft at a certain speed, and then the pin shaft will obtain a movement speed and impacts on the two lugs of the equivalent structure.

When coal gangue particles impact on the tail beam, according to equations (1)–(4), the normal force between them is

$$P_{PTn} = K_{PT} \cdot \delta_{PT}^{n} + D_{PT} \cdot \dot{\delta}_{PT}, \tag{9}$$

among which

$$\begin{aligned} K_{PT} &= \frac{4\sqrt{R_{PT}}}{3E_{PT}}, \\ E_{PT} &= \frac{1-\nu_P^2}{E_P} + \frac{1-\nu_T^2}{E_T}. \end{aligned} \tag{10}$$

The contact surface of the tail beam can be equivalent to a sphere with an infinite radius, i.e., $R_{TM} \longrightarrow \infty$, so the equivalent contact radius between coal gangue particles and the tail beam is

$$R_{PT} = R_P. \tag{11}$$

The tangential force when coal gangue impacts the tail beam is

$$P_{PTt} = f_{PT} \cdot P_{PTn}. \tag{12}$$

Therefore, the combined force between coal gangue and tail beam is

$$\left|P_{PT}\right| = \sqrt{\left(P_{PTn}\right)^2 + \left(P_{PTt}\right)^2} = \sqrt{1 + f_{PT}^2}\left|P_{PTn}\right|, \tag{13}$$

where $K_{PT}$, $E_{PT}$, and $f_{PT}$ are the contact stiffness, equivalent elastic modulus, and frictional coefficient between coal gangue particles and the tail beam, respectively, $R_P$ is the radius of coal gangue particles, $E_P$, $\nu_P$, and $E_T$, $\nu_T$ are the elastic modulus and Poisson's ratio of coal gangue particles and the tail beam, respectively, $\delta_{PT}$ is the normal contact compression between the particle and the tail beam, and $\dot{\delta}_{PT}$ is the normal instantaneous contact velocity between the particle and the tail beam.

If the force and motion at the clearance are uniform, according to equations (5)–(6), the contact stiffness between the tail beam and the pin shaft is

$$K_{Tz} = \frac{4\sqrt{R_{Tz}}}{3\pi E_{Tz}}, \tag{14}$$

in which

$$\begin{aligned} E_{Tz} &= \frac{1-\nu_T^2}{E_T} + \frac{1-\nu_z^2}{E_z}, \\ R_{Tz} &= \frac{R_T R_z}{R_T - R_z}. \end{aligned} \tag{15}$$

The normal and tangential contact forces between the tail beam and the pin shaft are

$$\begin{aligned} F_{Tzn} &= K_{Tz} \cdot \delta_{Tz}^{n} + D_{Tz} \cdot \dot{\delta}_{Tz}, \\ F_{Tzt} &= -c_{fTz} c_{dTz}\left(K_{Tz} \cdot \delta_{Tz}^{n} + D_{Tz} \cdot \dot{\delta}_{Tz}\right)\mathrm{sgn}\left(v_{Tt}\right). \end{aligned} \tag{16}$$

Based on this, the value of the total force between the tail beam and the pin shaft is

$$\left|F_{Tz}\right| == \sqrt{1 + \left[c_{fTz} c_{dTz}\mathrm{sgn}\left(v_{Tt}\right)\right]^2}\left|F_{Tzn}\right|, \tag{17}$$

where $D_{Tz}$ and $E_{Tz}$ are the coefficient of restitution and equivalent elastic modulus between the tail beam and the pin shaft, $R_T$ and $R_z$ are the radii of the tail beam shaft hole and the pin shaft, $E_z$ and $\nu_z$ are the elastic modulus and the Poisson's ratio of the pin shaft, $\delta_{Tz}$ is the normal contact compression between the tail beam and the pin shaft, $\dot{\delta}_{Tz}$ is the normal instantaneous contact velocity between the tail beam and the pin shaft, $c_{dTz}$ is the dynamic correction coefficient of tail beam and the pin shaft, $c_{fTz}$ is the frictional coefficient between the tail beam and the pin shaft, and $v_{Tt}$ is the instantaneous tangential relative contact velocity between the tail beam and the pin shaft.

Under the action of the tail beam, the unilateral normal and tangential contact forces between the pin shaft and the equivalent structure are

$$\begin{aligned} F_{zEn} &= K_{zE} \cdot \delta_{z}^{n} + D_{zE} \cdot \dot{\delta}_{z}, \\ F_{zEt} &= -c_{fzE} c_{dzE}\left(K_{zE} \cdot \delta_{z}^{n} + D_{zE} \cdot \dot{\delta}_{z}\right)\mathrm{sgn}\left(v_{zEt}\right). \end{aligned} \tag{18}$$

Based on this, the value of the total force between the pin shaft and the equivalent structure is

$$\left|F_{Tz}\right| = 2 \cdot \sqrt{1 + \left[c_{fzE} c_{dzE}\mathrm{sgn}\left(v_{zEt}\right)\right]^2}\left|F_{zEn}\right|. \tag{19}$$

Among them, contact stiffness between the pin shaft and the equivalent structure is

$$K_{zE} = \frac{4\sqrt{R_{zE}}}{3\pi E_{zE}}, \tag{20}$$

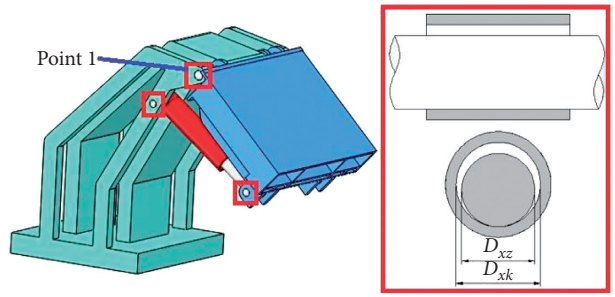


Figure 2: Tail beam structure and its radial clearance structure.

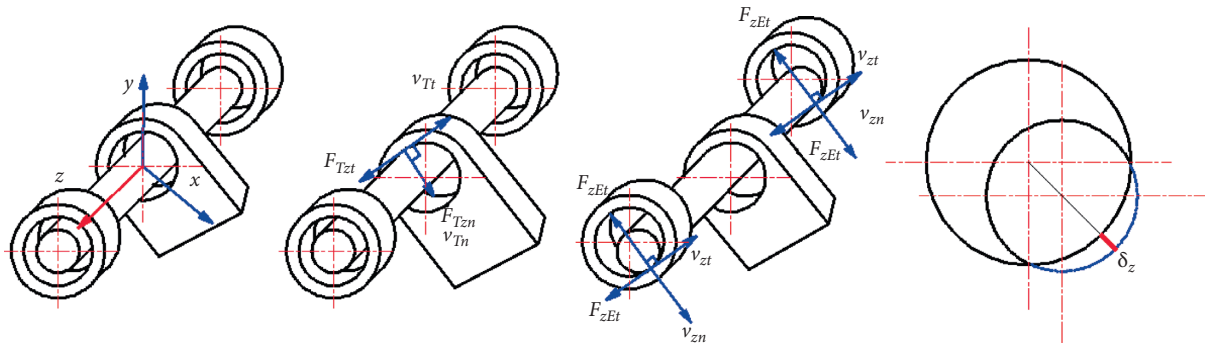


Blue indicator lines are in the xy plane

Figure 3: Contact process of the single independent clearance point 1.

in which

$$E_{zE} = \frac{1-\nu_z^2}{E_z} + \frac{1-\nu_E^2}{E_E},$$
$$R_{zE} = \frac{R_z R_E}{R_E - R_z}, \tag{21}$$

where $D_{zE}$ and $E_{zE}$ are the coefficient of restitution and equivalent elastic modulus of the tail beam and the pin shaft, $R_E$ is the radius of the pin shaft hole of the equivalent structure, $E_E$ and $\nu_E$ are the elastic modulus and Poisson's ratio of the equivalent structure, $\delta_z$ is the normal contact compression of the pin shaft and the equivalent structure, $\dot{\delta}_z$ is the normal instantaneous contact velocity between the pin shaft and the equivalent structure, $c_{dz\,E}$ is the dynamic correction coefficient of pin shaft and equivalent structure, $c_{fzE}$ is the frictional coefficient between the pin shaft and the equivalent structure, and $v_{zEt}$ is the instantaneous tangential contact velocity between the pin shaft and the equivalent structure.

If only a single clearance at the tail beam structure is considered, its first contact process and the contact force model can be described above. However, the tail beam structure is axisymmetric. There are three clearance connection units on each side and six clearance connection units in total. When coal gangue impacts on the axle wire of the upper metal plate of the tail beam, as we can learn from Figure 4, the load of the different contact points (such as contact-p1, contact-p2, and contact-p3 and contact-p4, contact-p5, and contact-p6) is different, which will cause the nonuniform motion of the pin shaft. It is difficult to estimate the nonhomogeneous forces and the nonhomogeneous motion of the pin shaft, so it is difficult to describe and model it theoretically. This is the first difficulty in the theoretical research of the impact contact behavior between coal gangue and the clearance-contained tail beam structure.

Meanwhile, the structure contains multiple clearances: the contact behaviors among the multiple clearances will affect each other, which further increases the complexity and difficulty of the theoretical modeling of the multiple clearances-contained tail beam structure, and it is difficult to clearly differentiate its motion and action stages. This is the second difficulty in the theoretical research of the system impact contact behavior.

Finally, the interaction forces of the clearance connection element cannot be consumed by a single collision; thus, the contact between the different parts of the clearance does not just happen once and end, but in a short continuous process of contact. Each clearance connection unit is composed of the pin shaft and the other two parts, but the contact between the pin shaft and the other two parts is not synchronized. Every reciprocating contact behavior will accompany the change of the contact position and contact status, and the complex change of the contact pair number and continuous contact number caused the unpredictability in the state of the system response after the multiple clearances-contained tail beam structure is impacted by coal gangue. This is the third difficulty in the theoretical research of the system impact contact behavior.

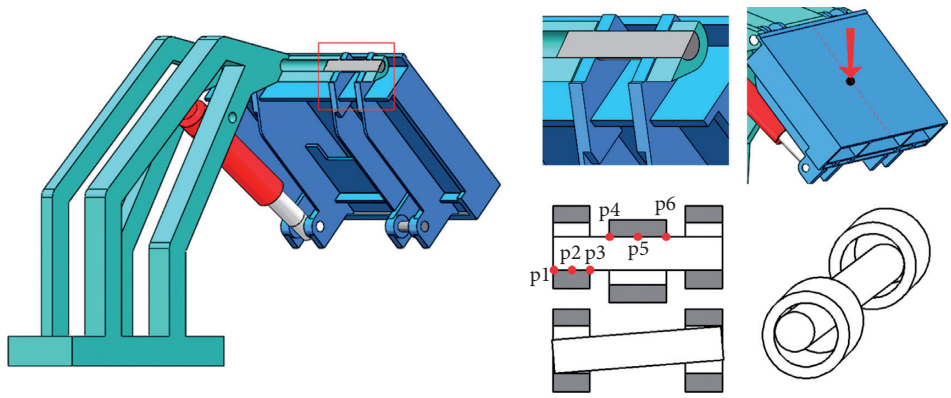


Figure 4: The nonuniform force and disorderly motion of the pin shaft.

From the above analysis, it is extremely difficult to analyze the interaction between coal gangue and the multiple clearances-contained tail beam structure theoretically.

## 3. Establishment of the Impact Contact Simulation Model between Coal Gangue and the Clearance-Contained Tail Beam Structure

Contact behavior and interaction process between coal gangue and the clearance-contained tail beam structures are complex, which leads to the difficulty of its theoretical solution. However, it is inevitable that there are many clearances in the tail beam structure during assembly. If it is equivalent to the two-dimensional plane mechanism to the theoretical modeling, though it can be realized, the working conditions are too simplified and idealized and the calculation results of the plane model are too deviated from the actual conditions. At the same time, in the impact and contact process between coal gangue and tail beam or the different parts of the clearance, it is accompanied by the local large deformation at the contact position of the contactants, rapid increasing and strengthening of the transient stress, and compression vibration of the hydraulic oil in the cylinder, etc. These complex real behaviors will be ignored in the theoretical process; therefore, even if it is possible to build a theoretical model, the pure theoretical calculation results are also not accurate. The finite element contact analysis can consider more factors than the theoretical modeling in the process of contact; contact parameters between the contact objects such as contact stiffness in the finite element will change in real time with the continuation of the contact process; and it can solve and simulate the unascertainable problems in the contact process such as the contact interface size, position, contact state, and contact conditions in the contact process of the transient impact and can effectively simulate the local large deformation and mechanical characteristics of the contact area. With the advantage of virtual reality, the dynamic impact contact process of the 3D stereoscopic structure model between coal gangue and the multiclearances-contained tail beam structure can be simulated and analyzed more precisely. Based on the realization difficulty of the theoretical modeling and solution, the finite element contact simulation method is adopted to analyze the system impact contact behavior of the multiclearance structure in this paper.

In order to clarify the influence law of the pin shaft radial assembly clearances on the dynamic response of the tail beam structure after the impact of coal gangue under the impact dynamic load, this section will carry out the impact contact simulation analysis of coal gangue and the clearance-contained tail beam structure in the Abaqus simulation platform. The nonlinear contact behavior of the pin shaft and the contact response characteristics of the clearance-contained system induced by the impact of coal gangue on the tail beam structure under the conditions of multiple clearances and variable clearances will be studied.

The hydraulic oil in the tail beam jack has great influence on the system response. The parameters that have the greatest influence on the liquid under stress are the stiffness and damping of the liquid. The other parameters of the hydraulic oil certainly have an influence on its performance, but they have little influence on the impact contact response between coal gangue and the clearance-contained tail beam structure. It is extremely difficult to directly simulate the compression and give in to pressure characteristics of the liquid in the finite element software, but the spring damping module can realize the simulation of the compression and pressure boosting characteristics, force transfer, and vibration attenuation characteristics of the hydraulic oil. Therefore, in this paper, the tail beam jack is equivalent to the spring damping module with the same stiffness. In order to add the spring damping module, the main structure of the tail beam jack is cancelled, and only the top end of the piston rod and the bottom of the cylinder are retained. The simulation model of coal gangue and the clearance-contained tail beam structure is shown in Figure 5. A very small clearance is reserved between the sphere and the upper metal plate of the tail beam when modeling. The pin shaft and the pin shaft hole are defined as the center axis alignment. The 3D model is imported into Abaqus to mesh the model. The hexahedral mesh can improve the calculation accuracy. Therefore, the sphere and the upper metal plate of the tail beam and all the pin shafts

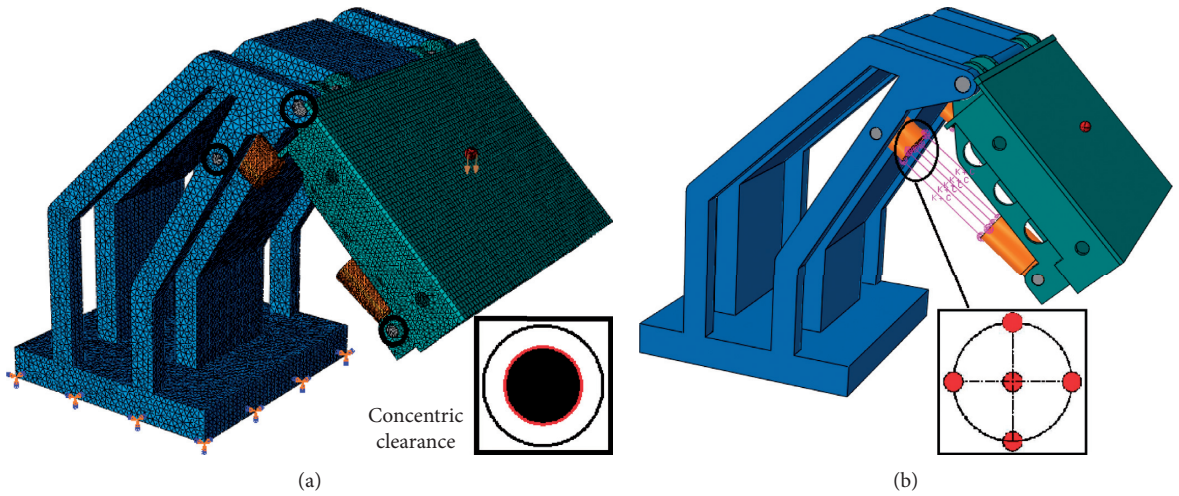


Figure 5: Finite element simulation model with multiclearance. (a) Mesh and boundary conditions. (b) Position of the spring and damping.

are divided into the hexahedral mesh. The remaining parts (including the equivalent structure) are divided into the tetrahedral meshes so as to save the simulation operation time. In order to reduce the coupling calculation difficulty of the finite element mesh and the equivalent spring between the end part and bottom part of the tail beam jack, the end part and the bottom part of the jack are both divided into the tetrahedral mesh. The model after the mesh is shown in Figure 5(a).

The material parameters for the sphere and the tail beam structure are defined, respectively. This paper aims to reveal the influence law of clearances on the nonlinear motion of the pin shaft, the impact contact response of the tail beam system, and the system response differences after coal gangue impact. The material properties are defined as elasticity. The specific parameters are shown in Table 1. The frictional coefficient between coal gangue and the tail beam is set to 0.3, and the frictional coefficient between the metal components is set to 0.2. Full constraints are imposed on the bottom surface of the equivalent structure, and the contact parameters are defined for the contact parts. The velocity of 7.668 m/s is applied to the sphere, and five spring damping modules are evenly arranged between the end face of the end part and the bottom part of the tail beam jack to simulate the deformation and force transmission of the tail beam jack under impact. The position of the spring is shown in Figure 5(b). Each spring has the same equivalent stiffness. The damping of the spring only changes the response time and has no influence on the response process, and in order to improve its stable speed, the spring damping coefficient is set to 12000.

The calculation model of the equivalent spring stiffness with constant stiffness $K_{Qw}$ and constant damping $c$ of the hydraulic cylinder is shown in Figure 6. Based on this, the equivalent stiffness model of the tail beam jack [42, 43] is

$$K_{Qw} = \frac{k_q \times k_g}{k_q + k_g} = \frac{S_H (D_d - d) E_{GT}}{S_H + l k_y (D_d - d) E_{GT}}. \quad (22)$$

Among them, $k_q$ is the stiffness of the hydraulic oil (high-pressure emulsion) inside the tail beam jack, $k_g$ is the stiffness of the cylinder body of the tail beam jack, $l$ is the height of the liquid column of the hydraulic oil inside the tail beam jack, and $k_y$ is the volume compression coefficient of the emulsion, $k_y = 1/E_r$.

After further simplification, the stiffness model in this paper can be calculated according to the following equation:

$$K_{Qw} = \frac{S_H (D_d - d) E_{GT} E_r}{S_H E_r + l (D_d - d) E_{GT}}. \quad (23)$$

## 4. System Impact Contact Dynamic Characteristics Analysis under the Conditions of Multiple Clearances and Variable Clearances

The radial clearance of the connecting unit is set between the tail beam and the tail beam jack and between the tail beam jack and the equivalent structure to be 0.75 mm. Radial clearances of the connecting unit between the tail beam and the equivalent structure are 0 mm, 0.25 mm, 0.5 mm, and 0.75 mm in diameter, respectively. Then, the contact simulation when the structure with two clearances and the structure with three clearances are impacted by coal gangue was completed, respectively. Extracted the stress of the center spring, the stress of the pin shaft test point, the velocity and acceleration data of the tail beam test point, respectively, and the positions of the selected test points are shown in Figure 7.

After the impact of coal particles, the changing curves of the spring stress, the stress of the pin shaft test point, and the velocity and acceleration of the tail beam test point within the simulation time of 0.261 s are shown in Figures 8–11, respectively.

When the radial clearance between the tail beam and the equivalent structure is 0, the stress of the pin shaft test point increases rapidly during the initial operation stage of the simulation and then gradually decreases. When there is a clearance at the connecting unit, the stress of the pin shaft test point hardly changes during the initial operation stage, but the stress value

Table 1: Material properties of the simulation model with clearance.

| Material | Density ($kg \cdot m^{-3}$) | Elastic modulus (GPa) | Poisson's ratio |
|---|---|---|---|
| Coal | 1380 | 2.20 | 0.28 |
| Gangue | 2800 | 34 | 0.3 |
| Tail beam structure | 7850 | 206 | 0.3 |
| Tail beam Jack | 7890 | 209 | 0.269 |

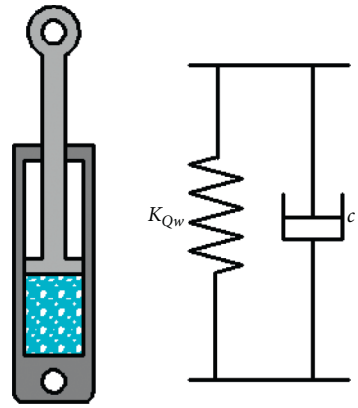


Figure 6 Equivalent spring stiffness of the hydraulic cylinder.

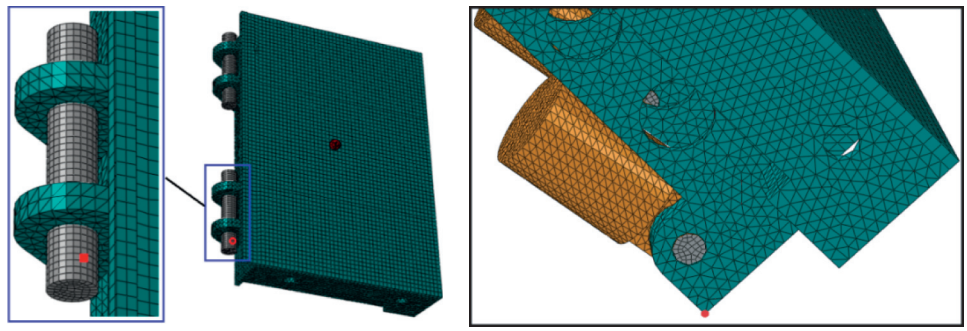

(a) (b)

Figure 7: Test point positions of (a) pin shaft and (b) tail beam.

changes suddenly at a certain moment. At this time, the pin shaft collides with the inner hole surface of the pin shaft hole at the test point. When the radial clearance of the connecting unit between the tail beam and the equivalent structure increases from 0 to 0.25 mm, i.e., the structure changes from 2-clearance state to 3-clearance state, the overall fluctuation amplitude of the spring stress, the stress amplitude of the pin shaft test point, and the acceleration and velocity amplitude of the tail beam test point are all reduced. At 3-clearance state, as the radial clearance between the tail beam and the equivalent structure connection unit changes, the contact time between the pin shaft test point and the inner hole surface of the pin shaft hole changes. As this clearance size increases, the spring stress, the stress of the pin shaft test point, and the velocity of the tail beam test point gradually increases, while the acceleration of the tail beam test point gradually decreases. The changing rule of the amplitude of the spring stress and the acceleration of the tail beam test point is not affected by the sudden change of the clearance. When the clearance size increases from 0 to 0.75 mm, the amplitude of the spring stress gradually increases, but the acceleration amplitude of the tail beam test point gradually decreases. Comparing the changing curves of the pin shaft test point and the velocity of the tail beam test point in 2-clearance and 3-clearance states, when the clearance size is 0.75 mm, the velocity amplitude of the tail beam test point in the 3-clearance state is greater than the corresponding contact response in the 2-clearance state. And when the clearance size in the 3-clearance state increases, the difference of the stress amplitude of the pin shaft test point between the 3-clearance state and the 2-clearance state gradually decreases. It can be seen that the dynamic characteristics of the system with clearances are affected by two factors, which are the number of the clearances and the size of the clearances. When the clearance size increases to a certain extent, it might compensate for the change of the system response law caused by the sudden change of the clearance number.

Figures 12–13 shows the contact response when coal gangue impacts the tail beam structure in the multi-clearance state, where the radial clearance between the

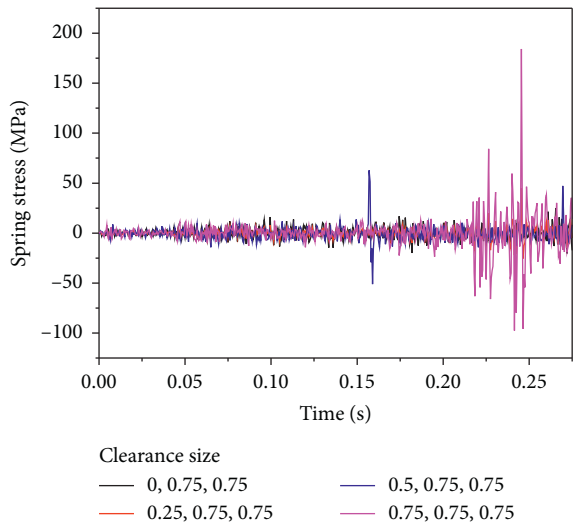


Figure 8: Spring stress.

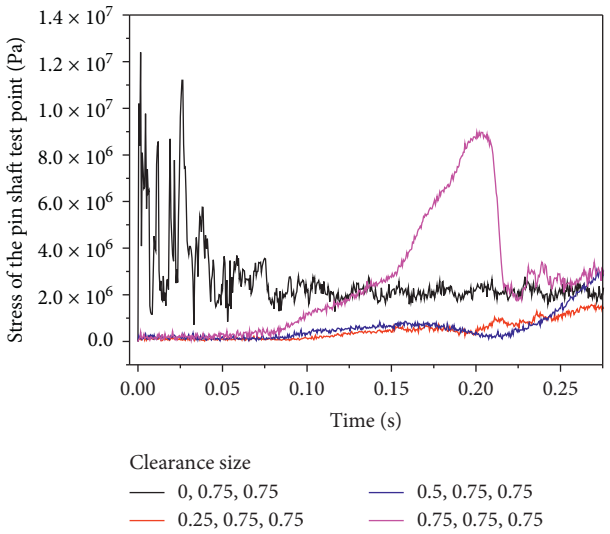


Figure 9: Stress of the test point of the pin shaft.

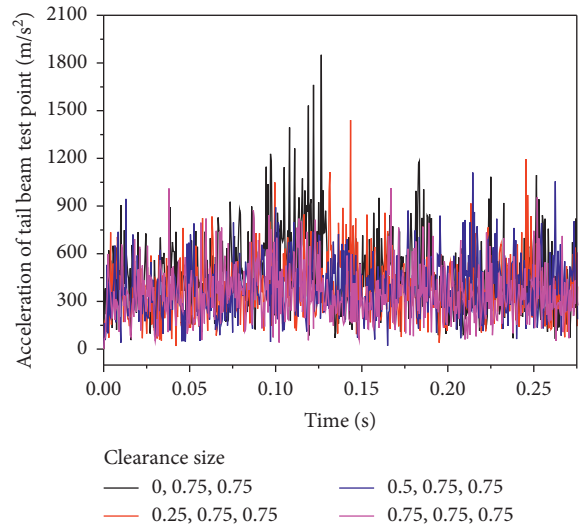


Figure 10: Acceleration of the tail beam test point.

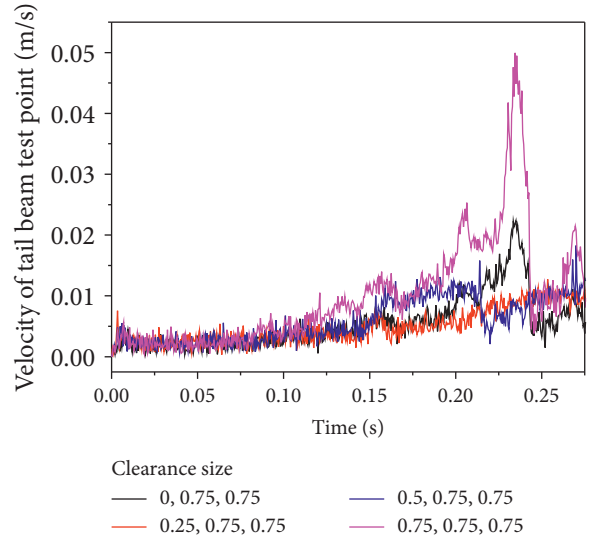


Figure 11: Velocity of the tail beam test point.

tail beam and the equivalent structure in 3-clearance state is 0.25 mm in diameter. It can be seen from the figures that spring stress and the pin shaft test point stress are greater than coal when gangue impacts on the tail beam under 2-clearance and 3-clearance states. In 2-clearance state, the amplitude of the spring stress during coal and gangue impact is 21.4815 MPa and 75.7795 MPa, respectively (Figure 12(a)), and the stress amplitude of the pin shaft test point is 12.4 MPa and 20.1 MPa, respectively (Figure 12(b)). The ultimate stresses obtained by the spring and the pin shaft test point when gangue impacts the tail beam are 3.5276 time and 1.621 time than that of coal, respectively, and the differences are 54.298 MPa and 7.7 MPa, respectively. In 3-clearance state, the spring stress amplitudes when coal and gangue impacts the tail beam are 44.94357 MPa and 106.869 MPa (Figure 13(a)), and the stress amplitudes of the pin shaft test point are 1.58 MPa and 2.18 MPa (Figure 13(b)). At this time, the ultimate stresses obtained by the spring and the pin shaft test point when gangue impacts the tail beam are 2.3778 time and 1.3797 time than that of coal, and the differences are 61.92543 MPa and 0.6 MPa, respectively. Based on this, it can be seen that when the clearance-contained tail beam structure is impacted by coal gangue, the contact characteristics within the clearance (i.e., pin shaft) are significantly different. The differences in the contact stress of the pin shaft will further cause the differences in the movement and vibration characteristics of the pin shaft in the pin shaft hole. Therefore, the vibration response of the pin shaft can be taken as one coal gangue recognition parameter. With the sudden change of the system from 2-clearance state to 3-clearance state, the difference in spring stress amplitude during coal gangue impact increases slightly and the difference in stress

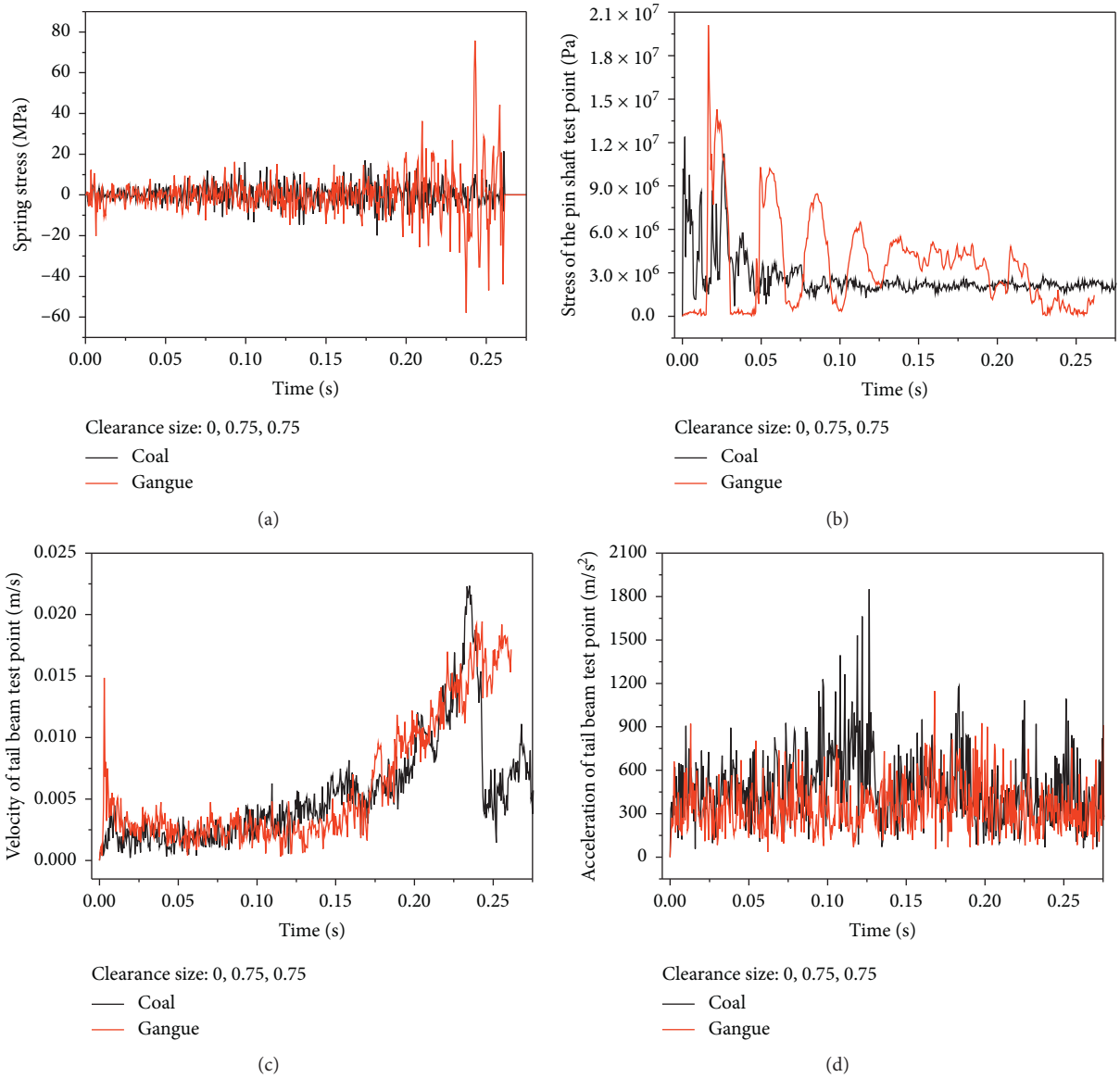


FIGURE 12: Impact contact response difference of the 2-clearance system. (a) Spring stress. (b) Stress of the pin shaft test point. (c) Velocity of the tail beam test point. (d) Acceleration of the tail beam test point.

amplitude of the pin shaft test point decreases. The ratio of the differences of the stress amplitude at the spring and pin shaft test point when coal gangue impacted is both reduced.

From the velocity and acceleration curves of the tail beam test point in the figure, it can be seen that, in the entire simulation stage, the difference of the velocity and acceleration of the tail beam test point after coal gangue impact between 2-clearance state and 3-clearance state shows the opposite trend. The amplitude and variation range of the velocity at the tail beam test point after the impact of gangue under 2-clearance state is both smaller than that of coal. However, the amplitude and variation range of the velocity at the tail beam test point under 3-clearance state after gangue impact is greater than that of coal. The overall value and amplitude of the acceleration at the tail beam test point after the impact of gangue under 2-clearance state are smaller than that of coal, while the overall value and amplitude of the acceleration at the tail beam test point after the gangue under 3-clearance state are greater than that of coal. From the overall view, the law of differences of tail beam after the impact of coal gangue under multiple clearances does not seem to be uniform. However, the impact contact between coal gangue and the tail beam is completed within a very short time in the initial stage of the simulation, and the movement and dynamic responses of the tail beam caused by the impact of coal gangue should be studied in this time period. Taking the dynamic responses of the tail beam within 0.02 s as the research objects, in 2-clearance state, when coal gangue impacts the tail beam, the velocity amplitudes of the tail beam test point are 0.00449 m/s and 0.01486 m/s, respectively (Figure 12(c)) and the acceleration amplitudes are

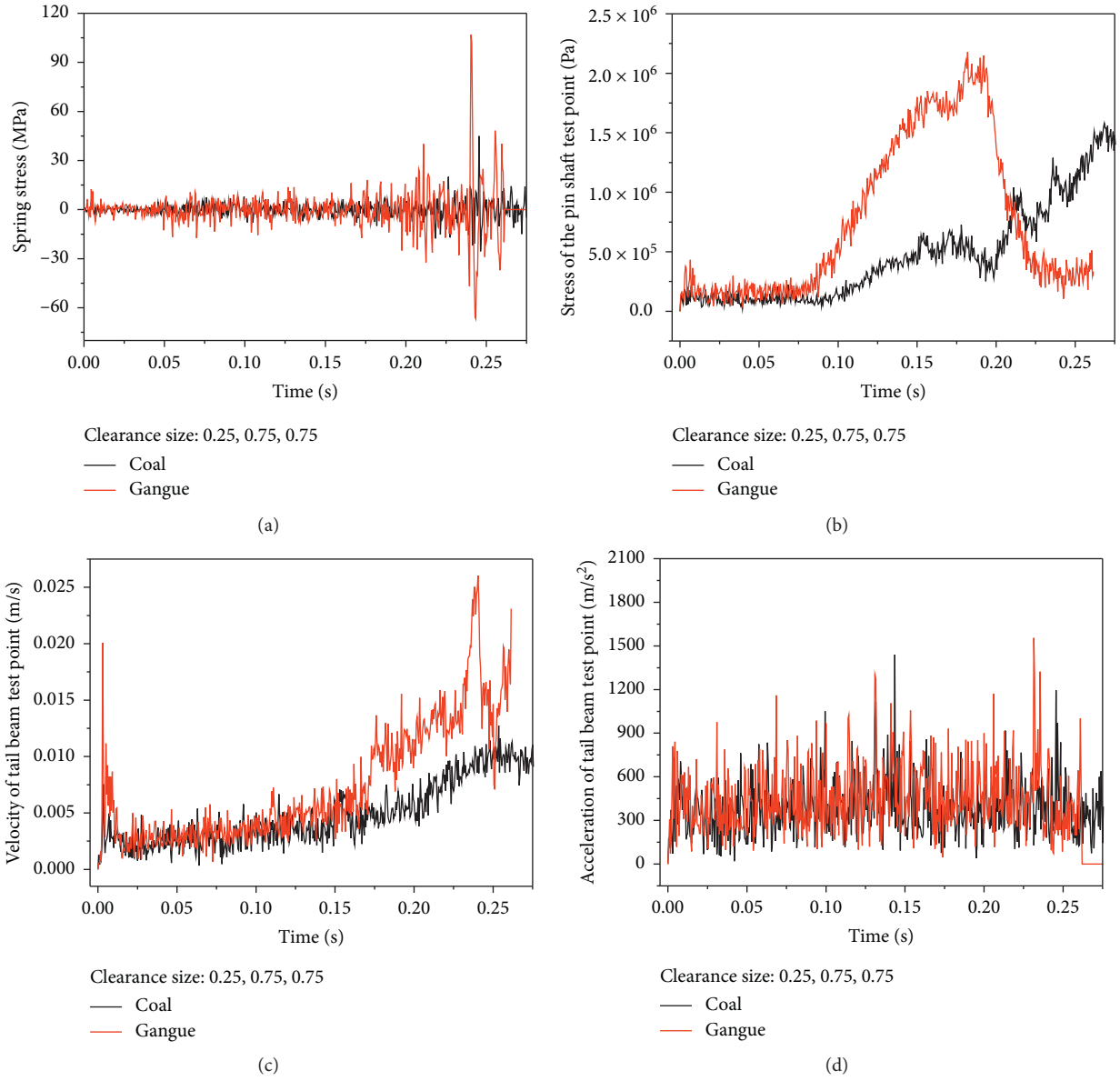


Figure 13: Impact contact response difference of the 3-clearance system. (a) Spring stress. (b) Stress of the pin shaft test point. (c) Velocity of the tail beam test point. (d) Acceleration of the tail beam test point.

907.255 m/s$^2$ and 921.489 m/s$^2$, respectively (Figure 12(d)). When gangue impacts the tail beam, the velocity and acceleration amplitudes obtained by the tail beam are 3.3096 times and 1.0157 time than that of the coal and the differences are 0.14411 m/s and 14.234 m/s$^2$, respectively. In 3-clearance state, the velocity amplitudes of the tail beam test point are 0.00755 m/s and 0.02007 m/s, respectively (Figure 13(c)) and the acceleration amplitudes are 735.254 m/s$^2$ and 841.027 m/s$^2$, respectively (Figure 13(d)). The velocity and acceleration amplitudes obtained by the tail beam when impacted by gangue are 2.6583 times and 1.1439 time than that of coal and the differences are 0.01252 m/s and 105.773 m/s$^2$, respectively. According to this, it can be seen that the velocity and acceleration amplitude obtained by the tail beam test point when gangue impacts in the multiclearance state are both greater than that of coal. Among them, as the system changes from 2-clearance state to 3-clearance state, the difference in velocity amplitude of the tail beam test point when impacted by coal gangue decreases slightly, and the difference in acceleration amplitude increases significantly. The ratio of the difference in velocity amplitude of the tail beam test point decreases, but the ratio of the difference in acceleration amplitude increases.

The obtained data also show that when the same particle impacts the two clearance-contained tail beam structure and three clearance-contained tail beam structure, the amplitude of the stress obtained by the spring and the amplitude of the vibration velocity at the test point of the tail beam with 3-clearance state are both

greater than that with 2-clearance state. That is, after the system changes from two clearances to three clearances, the bearing load required by the tail beam jack and the vibration velocity of the tail beam of the three-clearance system increases under the same impact statement. According to this, the increase in the number of the clearance will reduce the stability of the system, increase the pressure supply requirements for the tail beam jack, and thus reduce the working performance of the hydraulic support. In order to improve the working performance of the support, the clearance should be controlled.

## 5. Conclusions

As the multibody assembly device, multiple forms of clearance exist in the hydraulic support structure. However, the effect of its presence on the manufacturing and performance of the hydraulic supports has never been studied. In order to clearly grasp the dynamic response between coal gangue and the tail beam structure, the nonlinear factor of clearance is introduced for the first time in the relevant research of the hydraulic support, and then the impact contact behavior between coal gangue and the radial clearance-contained tail beam structure is studied. The following conclusions can be drawn:

(1) Through the theoretical analysis for the impact contact behavior between coal gangue and the multiclearance-contained tail beam structure, it is extremely difficult to research the system interaction by the theoretical modeling and solution, and the finite element contact simulation is selected as the research method.

(2) Under the condition that the other two clearances were 0.75 mm, the finite element impact contact simulation was carried out for the clearance between the tail beam and the equivalent structure is 0, 0.25 mm, 0.5 mm, and 0.75 mm, respectively. When the radial clearance of the connection unit between the tail beam and the equivalent structure increases from 0 to 0.25 mm, the overall fluctuation amplitude of the spring stress, the stress amplitude of the pin shaft test point, and the acceleration and velocity amplitudes of the tail beam test point all decrease.

(3) In 3-clearance state, with the increase of the radial clearance size of the connection unit, the spring stress, the stress of the pin shaft test point, and the velocity of the tail beam test point gradually increase, but the acceleration of the tail beam test point gradually decreases.

(4) Comparing 2-clearance and 3-clearance state, the velocity amplitude of the tail beam test point under the 3-clearance state when the clearance size is 0.75 mm is greater than the corresponding contact response in 2-clearance state, and the difference of the stress amplitude of the pin test point between 3-clearance state and 2-clearance state decreases gradually with the increase of the clearance size of 3-clearance state.

(5) In the condition of multiclearance, the amplitudes of the spring stress, the stress of the pin shaft test point, and the velocity and acceleration obtained by the test point of the tail beam when gangue is impacted are all greater than that of coal. The contact difference in pin shaft is obvious, which can be used as coal gangue distinguishing parameter.

(6) When the same particle impacts the tail beam structure, the amplitude of the spring stress and the amplitude of the vibration velocity at the test point of the tail beam with 3-clearance state are both greater than that with 2-clearance state. The increase in the number of the clearance will reduce the system stability and increase the pressure supply requirements for the tail beam jack and reduce the working performance of the hydraulic support.

The research will provide the theoretical basis for the clearance-contained hydraulic support.

## Data Availability

The data used to support the findings of this study are included within the article.

## Additional Points

(1) The clearance is introduced into the related research of the hydraulic for the first time, and the influence of clearance to the system contact responses is studied

(2) Impact contact simulation between coal gangue and the multiple and variable clearance-contained tail beam structure is carried out, and contact response difference after coal gangue impact is compared with different clearances system

## Conflicts of Interest

The authors declare no conflicts of interest.

## Acknowledgments

This work was supported by the National Natural Science Foundation of China (Grant no. 51974170) and Special Funds for Climbing Project of Taishan Scholars.

## References

[1] Y. X. Xu, G. F. Wang, M. Z. Li, Y. J. Xu, H. J. Han, and J. H. Zhang, "Investigation on coal face slabbed spalling features and reasonable control at the longwall face with super large cutting height and longwall top coal caving method," *Journal of China Coal Society*, 2020.

[2] M. Witek and S. Prusek, "Numerical calculations of shield support stress based on laboratory test results," *Computers and Geotechnics*, vol. 72, pp. 74–88, 2016.

[3] X. Wang, Z. Yang, J. Feng, and H. Liu, "Stress analysis and stability analysis on doubly-telescopic prop of hydraulic support," *Engineering Failure Analysis*, vol. 32, pp. 274–282, 2013.

[4] S. R. Xie, L. Wang, D. D. Chen, E. Wang, H. Li, and S. S. He, "Spatial load-bearing characteristics of four-pillar chock-shield support [J]," *Advanced Engineering Sciences*, vol. 52, no. 1, pp. 56–65, 2020.

[5] X. Zhao, F. Li, Y. Liu, and Y. Fan, "Fatigue behavior of a box-type welded structure of hydraulic support used in coal mine," *Materials*, vol. 8, no. 10, pp. 6609–6622, 2015.

[6] X. Ge, J. Xie, X. Wang, Y. Liu, and H. Shi, "A virtual adjustment method and experimental study of the support attitude of hydraulic support groups in propulsion state," *Measurement*, vol. 158, Article ID 107743, 2020.

[7] G. F. Wang, X. P. Hu, X. H. Liu et al., "Adaptability analysis of four-leg hydraulic support for underhand working face with large mining height of kilometer deep mine," *Journal of China Coal Society*, vol. 45, no. 3, pp. 865–875, 2020.

[8] E. Guan, H. Miao, P. Li, J. Liu, and Y. Zhao, "Dynamic model analysis of hydraulic support," *Advances in Mechanical Engineering*, vol. 11, no. 1, pp. 168781401882014–168781401882018, 2019.

[9] Z. Tian, S. Jing, S. Gao, and J. Zhang, "Establishment and simulation of dynamic model of backfilling hydraulic support with six pillars," *Journal of Vibroengineering*, vol. 22, no. 3, pp. 486–497, 2020.

[10] D. Szurgacz and J. Brodny, "Analysis of the influence of dynamic load on the work parameters of a powered roof support's hydraulic leg," *Sustainability*, vol. 11, no. 9, p. 2570, 2019.

[11] K.-L. Ting, J. Zhu, and D. Watkins, "The effects of joint clearance on position and orientation deviation of linkages and manipulators," *Mechanism and Machine Theory*, vol. 35, no. 3, pp. 391–401, 2000.

[12] X. Wang, W. Lin, X. Ji, Z. Gao, X. Bai, and Y. Guo, "Dynamic analysis of a planar multibody system with multiple revolute clearance joints," *Proceedings of the Institution of Mechanical Engineers, Part C: Journal of Mechanical Engineering Science*, vol. 233, no. 10, pp. 3429–3443, 2019.

[13] J. Chunmei, Q. Yang, F. Ling, and Z. Ling, "The non-linear dynamic behavior of an elastic linkage mechanism with clearances," *Journal of Sound and Vibration*, vol. 249, no. 2, pp. 213–226, 2002.

[14] X. Yang, J. Wang, and B. Li, "Dynamics modeling and simulation of RSSR spatial mechanism with spherical clearance joint," *Journal of Harbin Institute of Technology*, vol. 50, no. 7, pp. 73–79, 2018.

[15] P. Flores and J. Ambrósio, "Revolute joints with clearance in multibody systems," *Computers &Structures*, vol. 82, no. 17–19, pp. 1359–1369, 2004.

[16] J. Zhang, H. D. Yu, L. Li et al., "Dynamic performance analysis for over-constrained mechanisms with multiple revolute clearance joints," *Machine Design and Research*, vol. 34, no. 1, pp. 76–81+86, 2018.

[17] H. D. Zhang, "Researches on dynamics of planar parallel mechanisms considering the influence of joint clearance," *Degree of Doctor of Philosophy*, South China University of Technology, Guangzhou, China, 2019.

[18] T.-N. Shiau, Y.-J. Tsai, and M.-S. Tsai, "Nonlinear dynamic analysis of a parallel mechanism with consideration of joint effects," *Mechanism and Machine Theory*, vol. 43, no. 4, pp. 491–505, 2008.

[19] J. Li, H. Huang, S. Yan, and Y. Yang, "Kinematic accuracy and dynamic performance of a simple planar space deployable mechanism with joint clearance considering parameter uncertainty," *Acta Astronautica*, vol. 136, pp. 34–45, 2017.

[20] S. Erkaya and İ. Uzmay, "Experimental investigation of joint clearance effects on the dynamics of a slider-crank mechanism," *Multibody System Dynamics*, vol. 24, no. 1, pp. 81–102, 2010.

[21] X. Zhang, X. Zhang, and Z. Chen, "Dynamic analysis of a 3-RRR parallel mechanism with multiple clearance joints," *Mechanism and Machine Theory*, vol. 78, no. 78, pp. 105–115, 2014.

[22] X. S. Qiu, Z. B. Ren, P. Gui, and Y. K. Wei, "Dynamic modeling and simulation of a flexible deployable solar array with multiple clearances," *Journal of Astronautics*, vol. 39, no. 7, pp. 724–731, 2018.

[23] Z. Song, "Research on dynamics and control of planar parallel mechanisms with clearance joints," *Degree of Doctor of Philosophy*, Harbin Institute of Technology, Shenzhen, China, 2019.

[24] Y. Gu, Y. L. Zhang, J. L. Zhao, and S. Z. Yan, "Dynamic characteristics of free-floating space manipulator with joint clearance," *Journal of Mechanical Engineering*, vol. 55, no. 3, pp. 99–108, 2019.

[25] H. Wang, Y. J. Wang, and G. H. Zhao, "Structural optimization design of protection safety valve of coal mining hydraulic system," *Computer Simulation*, vol. 35, no. 1, pp. 394–397, 2018.

[26] W. Deng, J. Xu, Y. Song, and H. Zhao, "Differential evolution algorithm with wavelet basis function and optimal mutation strategy for complex optimization problem," *Applied Soft Computing*, Article ID 106724, 2020.

[27] Y J Song, D Q Wu, A W Mohamed, X B Zhou, B Zhang, and W Deng, "Enhanced success history adaptive DE for parameter optimization of photovoltaic models," *Complexity*, vol. 2020, Article ID 6660115, 2020.

[28] W. Deng, J. Xu, X.-Z. Gao, and H. Zhao, "An enhanced MSIQDE algorithm with novel multiple strategies for global optimization problems," *IEEE Transactions on Systems, Man, and Cybernetics: Systems*, pp. 1–10, 2020.

[29] Y J Song, D Q Wu, W Deng et al., "MPPCEDE: Multi-population parallel co-evolutionary differential evolution for parameter optimization," *Energy Conversion and Management*, vol. 228, Article ID 113661, 2021.

[30] H. M. Lankarani and P. E. Nikravesh, "A Contact Force Model With hysteresis Damping for Impact Analysis of Multibody Systems," *Journal of Mechanical Design*, vol. 112, no. 3, pp. 369–376, 1990.

[31] H M Lankarani and P Nikravesh, "Continuous contact force models for impact analysis in multibody systems," *Nonlinear Dynamics*, vol. 5, pp. 193–207, 1994.

[32] P. Flores, M. Machado, M. T. Silva, and J. M. Martins, "On the continuous contact force models for soft materials in multibody dynamics," *Multibody System Dynamics*, vol. 25, no. 3, pp. 357–375, 2011.

[33] M. R. Brake, "An analytical elastic-perfectly plastic contact model," *International Journal of Solids and Structures*, vol. 49, no. 22, pp. 3129–3141, 2012.

[34] M. R. W. Brake, "An analytical elastic plastic contact model with strain hardening and frictional effects for normal and oblique impacts," *International Journal of Solids and Structures*, vol. 62, pp. 104–123, 2015.

[35] Y. Yang, Q. Zeng, and L. Wan, "Dynamic response analysis of the vertical elastic impact of the spherical rock on the metal plate," *International Journal of Solids and Structures*, vol. 158, pp. 287–302, 2019.

[36] T Yu and J Y Chen, "Study of the Dynamic Characteristics of Mechanisms with all Clearance Joints," *Machinery Design & Manufacture*, no. 4, pp. 19–22, 2018.

[37] C. Brutti, G. Coglitore, and P. P. Valentini, "Modeling 3D revolute joint with clearance and contact stiffness," *Nonlinear Dynamics*, vol. 66, no. 4, pp. 531–548, 2011.

[38] Z. F. Bai, Y. Zhao, and Z. G. Zhao, "Dynamic characteristics of mechanisms with joint clearance," *Journal of Vibration and Shock*, vol. 30, no. 11, pp. 17–20+41, 2011.

[39] S. M. Varedi-Koulaei, H. M. Daniali, M. Farajtabar, B. Fathi, and M. Shafiee-Ashtiani, "Reducing the undesirable effects of joints clearance on the behavior of the planar 3-RRR parallel manipulators," *Nonlinear Dynamics*, vol. 86, no. 2, pp. 1007–1022, 2016.

[40] Y. Yang, J. J. R. Cheng, and T. Zhang, "Vector form intrinsic finite element method for planar multibody systems with multiple clearance joints," *Nonlinear Dynamics*, vol. 86, no. 1, pp. 421–440, 2016.

[41] A. A. Olyaei and M. R. Ghazavi, "Stabilizing slider-crank mechanism with clearance joints," *Mechanism and Machine Theory*, vol. 53, pp. 17–29, 2012.

[42] X. K. Liu, Z. H. Zhao, and R. Zhao, "Study on dynamic features of leg applied to hydraulic powered support under bumping load," *Coal Science and Technology*, vol. 40, no. 12, pp. 66–70, 2012.

[43] L. R. Wan, B. Chen, Y. Yang, and Q. L. Zeng, "Dynamic response of single coal-rock impacting tail beam of top coal caving hydraulic support," *Journal of China Coal Society*, vol. 44, no. 9, pp. 2905–2913, 2019.